transonic

THE MEASURE OF BETTER RESULTS.

Common Applications of PV Loops

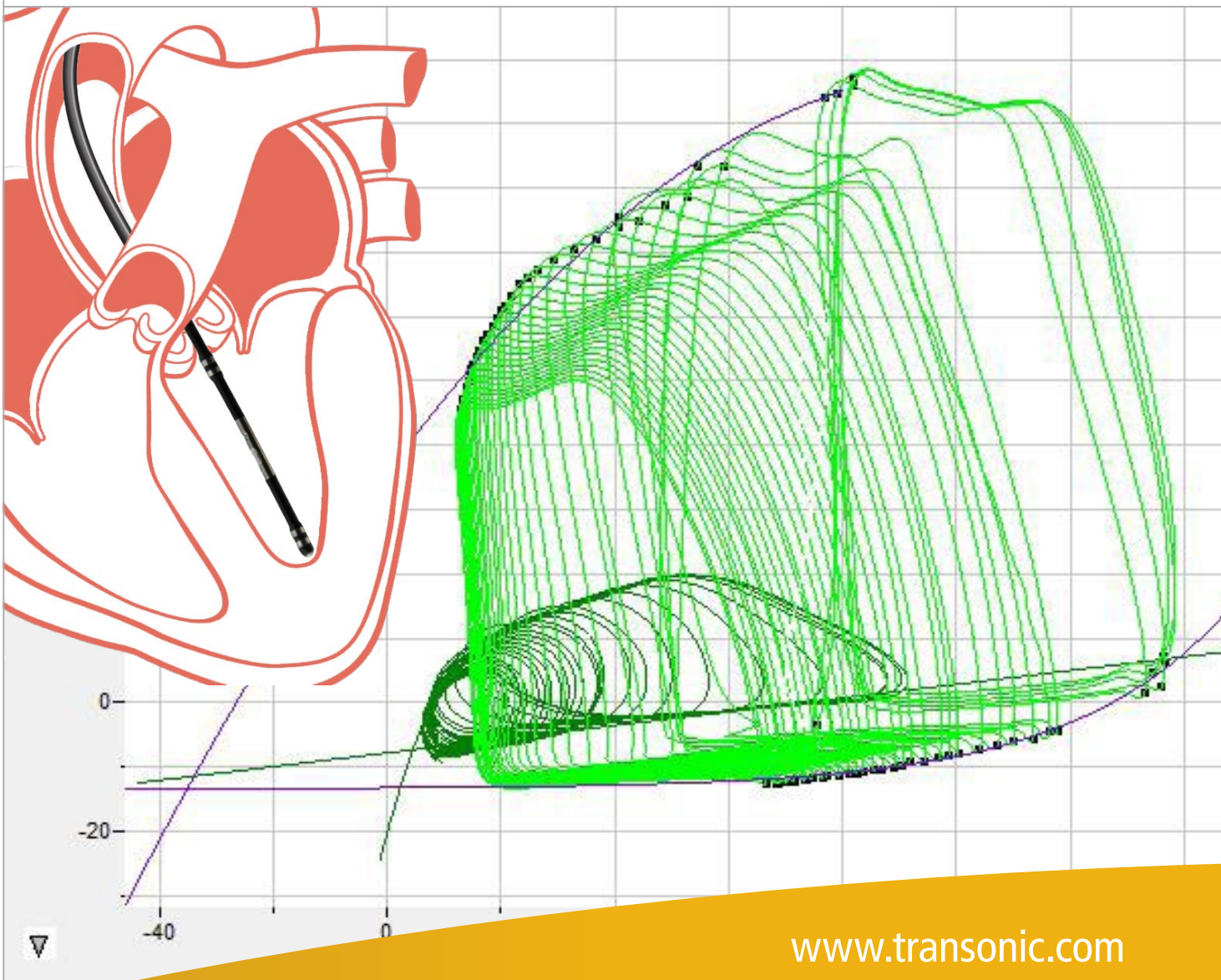

www.transonic.com

Table of Contents

Hemodynamics of Myocardial Infarction in Rodents 3
Translational Physiology of Myocardial Infarction 6
Hemodynamics of Cardiac Tissue Engineering 9
Hemodynamic Assessment in Safety Pharmacology 14
Right Ventricle Pressure-Volume Loops 16
Pulmonary Artery Hypertension & RV PV Loops 19

Hemodynamics of Myocardial Infarction in Rodents

When using invasive methods to measure hemodynamic parameters in rodents, most researchers studying chronic myocardial infarct are using permanent suture-induced descending coronary artery occlusion. Usually, they perform the Pressure-Volume (PV) Catheter study at 4 weeks (28 days) post-MI (3, 4, 8). Some researchers extend the artery occlusion study time another 2 weeks (1, 2) to study the effect of chronic heart failure/animal survival.

Cardiac remodeling at 28 days after the onset of MI is characterized by the structural changes of the LV having impact on whole heart, such as infarcted regional-wall thinning, chamber dilatation, and hypertrophy in the viable region. The severity of these changes are based on position of occlusion (1, 3, 7). Signs of early post-infarction remodeling taking place in a mouse heart are described in the table below. Due to strain-dependency and genetic background of animals and also, with the position of coronary artery occlusion, the post-MI mortality varies. For more information on factors related to MI models including cellular and genetic influence please see "Translational Physiology of Myocardial Infarction" on page 6.

STAGE POST-MI	BEGINNING	DEVELOPMENT	TIME FRAME	CHANGES OF MYOCARDIUM	VENTRICULAR MECHANICS	VENTRICULAR FUNCTION
Coronary artery occlusion	Acute ischemia	Infarct enlargement	Minutes - hours	Disorder of structural proteins	Passive myocardium	Impaired systolic function
Infarct stiffening	Necrosis progression	Collagen formation	Hours - days	Edema, necrosis, and degradation	Increased stiffness and strength; infarct expansion	Impaired systolic function
Collagen formation	Fibrosis	Decreasing collagen formation	7 - 28 days	Increase in collagen content (scar formation)	Maximum stiffness	Impaired diastolic function
Decreased collagen formation	Remodelling	Scar thinning; the rest of myocardium hypertrophy	28 days +	Scar shrinkage and collagen cross-linking	Decrease in stiffness; scar anisotropy	Improved LV function

*Post-infarction stages in mouse based on work of Shioura et. al. (1)

When cardiac hemodynamics are measured by PV catheterization at 4 weeks post-MI, the load dependent parameters of cardiac function (e.g. SV, SW, CO, EF, dP/dt max/min, Tau) are reduced as compared to intact animals (1). At the same time, compensatory hypertrophy of surviving myocardium occurs roughly up until 6 weeks post-MI, after which decompensation occurs. LV decompensation is marked by a significant decrease of developed pressure, strikingly reduced SV, SW and CO and development of diastolic dysfunction. A noticeable negative outcome of diastolic dysfunction is seen in the rise in end-diastolic pressure (EDP). It is also common for the left atrial and pulmonary venous pressures to elevate leading to pulmonary congestion and edema.

COMPARING MAJOR SYSTOLIC AND DIASTOLIC LOAD INDEPENDENT INDICES (CONTROL VS. POST-MI)

Systolic properties are characterized by the load-independent End Systolic Pressure-Volume Relationship (ESPVR) which is composed of the slope or end systolic elastance (Ees), and the volume axis intercept (V0). ESPVR can be characterized by either the quadratic or the linear equation. Generally, ESPVR is assumed to be influenced by afterload impedance (9), and when analyzed over wider ranges of contractile states, it was found to be non-linear (10) and the volume axis intercept is better estimated using quadratic rather than linear equation (11). For this reason when ESPVR (systolic functional contractility parameter) in rodents post-MI is compared to a control group, a simple t-test cannot be applied as it fails to account for covariance and statistical interdependence between Ees and V0. Therefore, it is best to report changes occurring in volume axis intercept (V0) and slope (Ees). To compare post-MI and control groups, analysis of covariance (ANCOVA) with dummy variable should be instituted (12). For further discussion of ESPVR comparison of groups see Burkhoff *et. al.* 2005 (13).

Hemodynamics of Myocardial Infarction Cont.

Diastolic properties are characterized by the load-independent End Diastolic Pressure-Volume Relationship (EDPVR). EDPVR is characterized by a non-linear curve fit of the change of ventricular pressure relative to change in ventricular volume (dP/dV). Post-MI changes characterized by an increase of collagen formation and scar cross-linking and shrinkage (see table) greatly influences final myocardial PV properties thus the position of the EDPVR . Slope of this relationship is called beta, also termed as chamber stiffness constant. When comparing EDPVR relationship post-MI one approach is to linearize it and use linear regression analysis with dummy variables or ANCOVA similar to ESPVR (12, 13).

As load independent parameters are measured, using pre-load reduction by temporary occlusion of inferior vena cava (IVC), a rightward shift of PV loops is observed. As a good internal control, it is imperative to select for analysis only those samples of IVC occlusion that were performed by similar technique including method of occlusion and vena cava location of preload reduction. Additionally, parameter such as ESPVR, EDPVR, time varying elastance (E_{max}), PRSW, dP/dt_{max} vs. EDV are all declining post-MI. PRSW (SW vs. EDV) deterioration reveals changes in systolic function independent of chamber geometry. Time-varying elastance indicates the LV chamber adjustments leading to decrease of compliance, defined by the proportionality between intraventricular pressure and volume. Left ventricular end-systolic elastance / effective arterial elastance increases at 4 weeks post MI indicating a worsening of this coupling ratio.

Using Admittance technique to assess load dependent and independent parameters in post-MI injured rodent heart has several distinct advantages over the traditional conductance method. There is no need for volume calibration of the catheter or hypertonic saline injection for parallel conductance determination with Admittance which saves time and reduces sources of error (6). By using Admittance method in rodent post-MI, an appropriate correction of the parallel conductance of injured cardiac muscle is achieved in real-time based on blood conductance calibrated to end systolic and end diastolic blood conductance and aortic flow. This occurs instantaneously while discarding the injured muscle parallel conductance (6). Admittance is also more insensitive to the impact of changes in heart geometry which may occur as a result of MI due to the ability to place the catheter in the center of the LV using Phase and Magnitude signals (5). See the PV Catheter Positioning Guide for placement methodology. Unguided conductance catheters can end up off-centered which gives inaccurate results (5).

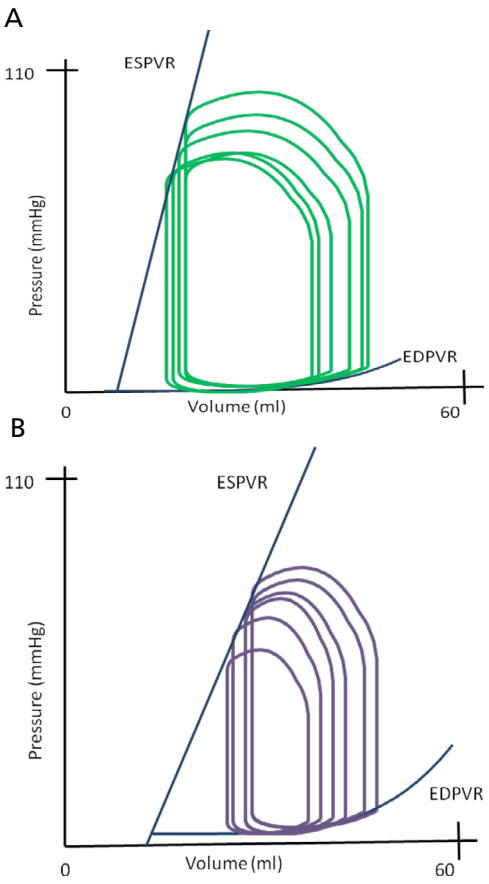

Representative drawing of load-independent PV loops post-IVC occlusion at (A) beginning of study (control) and (B) at 4 weeks post-MI. At 4 weeks post-MI the purple PV loops shows characteristic rightward shift with decreased slope of ESPVR. ESPVR is progressively worsening and continues to decline with time following MI. LV chamber remodelling post-MI leads to increased stiffness with decreased preload capacity during diastole as seen in changes to the EDPVR. The rise of EDP at 4 weeks post-MI leads to increased effort of LV muscle against which heart has to work during the filling phase. Additionally, rodents with healed infarcts operate at higher EDV at 6-10 weeks MI post as compared to healthy hearts.

Hemodynamics of Myocardial Infarction Cont.

REFERENCES

(1) Shioura KM, Geenen DL, Goldspink PH. "Assessment of cardiac function with the pressure-volume conductance system following myocardial infarction in mice." Am J Physiol Heart Circ Physiol 293: H2870–H2877, 2007.

(2) Patten RD, Aronovitz MJ, Deras-Mejia L, Pandian NG, Hanak GG, Smith JJ, Mendelsohn ME, Konstam MA. "Ventricular remodeling in a mouse model of myocardial infarction." Am J Physiol. 1998; 274:H1812–1820.

(3) Takagawa J, Zhang Y, Wong ML, Sievers RE, Kapasi NK, Wang Y, Yeghiazarians Y, Lee RJ, Grossman W, Springer ML. "Myocardial infarct size measurement in the mouse chronic infarction model: comparison of area- and length-based approaches." J Appl Physiol. 2007 Jun;102(6):2104-11.

(4) Chen J, Petrov A, Yaniz-Galende E, Liang L, de Haas HJ, Narula J, Hajjar RJ. "The impact of pressure overload on coronary vascular changes following myocardial infarction in rats." Am J Physiol Heart Circ Physiol. 2013 Mar 1;304(5):H719-28.

(5) Clark JE, Marber MS. "Advancements in pressure-volume catheter technology stress remodelling after infarction." Exp Physiol. 2013 Mar;98(3):614-21.

(6) Clark JE, Kottam A, Motterlini R, Marber MS. "Measuring left ventricular function in the normal, infarcted and CORM-3-preconditioned mouse heart using complex admittance-derived pressure volume loops." J Pharmacol Toxicol Methods. 2009 Mar-Apr;59(2):94-9.

(7) Ahn D, Cheng L, Moon C, Spurgeon H, Lakatta EG, Talan MI. "Induction of myocardial infarcts of a predictable size and location by branch pattern probability-assisted coronary ligation in C57BL/6 mice." Am J Physiol Heart Circ Physiol. 2004 Mar;286(3):H1201-7.

(8) van den Borne SW, van de Schans VA, Strzelecka AE, Vervoort-Peters HT, Lijnen PM, Cleutjens JP, Smits JF, Daemen MJ, Janssen BJ, Blankesteijn WM. "Mouse strain determines the outcome of wound healing after myocardial infarction." Cardiovasc Res. 2009 Nov 1;84(2):273-82.

(9) Burkhoff D, De Tombe PP, Hunter WC. "Impact of ejection on magnitude and time course of ventricular pressure-generating capacity." Am J Physiol. 1993 Sep;265(3 Pt 2):H899-909.

(10) Sato T, Shishido T, Kawada T, Miyano H, Miyashita H, Inagaki M, Sugimachi M, Sunagawa K. "ESPVR of in situ rat left ventricle shows contractility-dependent curvilinearity." Am J Physiol. 1998 May;274(5 Pt 2):H1429-34.

(11) Claessens TE, Georgakopoulos D, Afanasyeva M, Vermeersch SJ, Millar HD, Stergiopulos N, Westerhof N, Verdonck PR, Segers P. "Nonlinear isochrones in murine left ventricular pressure-volume loops: how well does the time-varying elastance concept hold?" Am J Physiol Heart Circ Physiol. 2006 Apr;290(4):H1474-83.

(12) Slinker BK, Glantz SA. "Multiple regression for physiological data analysis: the problem of multicollinearity." Am J Physiol. 1985 Jul;249(1 Pt 2):R1-12.

(13) Burkhoff D, Mirsky I, Suga H. "Assessment of systolic and diastolic ventricular properties via pressure-volume analysis: a guide for clinical, translational, and basic researchers." Am J Physiol Heart Circ Physiol. 2005 Aug;289(2):H501-12.

Translational Physiology of Myocardial Infarction

The main aspect of post-myocardial infarct/infarction (MI) research is to mimic conditions that lead to the development of myocardial ischemia. MI indicates irreversible myocardial injury resulting in necrosis of a significant portion of myocardium. Human clinical MI may be either of the non-reperfusion type, if the obstruction to blood flow is permanent, or the reperfusion type, if the obstruction is reversed after myocardial cell death. The infarct-affected areas are limited by distribution of the occluded vessel(s). In humans, the left main coronary artery occlusion generally results in a large antero-lateral and septum infarct, whereas occlusion of the left anterior descending coronary artery causes necrosis limited to the anterior wall. Hospital post-mortem findings in most cases reveal an acute thrombus overlying an atherosclerotic plaque in the coronary arteries. In these examples of vascular distribution, recreating this instance in animal research models has proved challenging due to the limitations caused by the fundamental difference between human and rodent cardiovascular physiology, carotid artery disease (CAD), and cellular and genetic makeup. Additionally, in the human population there is a known genetic polymorphism involving pathways of lipids, coagulation, and the renin-angiotensin system which does not currently have a known rodent analog.

CREATION OF RODENT MI MODEL

The natural development of MI stems from atherosclerosis (athero-gruel/sclerosis-hardening) plaque growth which occludes blood flow or suddenly ruptures. There is, however, difficulty in re-creating plaque growth in animal models which consistently leads to MI. Several diet supplementation methods have been used to simulate this natural disease progression. First, feeding cholesterol-rich diet can lead to chronic narrowing of coronary arteries and hypercholesterolemia, making them vulnerable to plaque buildup and thrombosis (1). Additionally, using mice lacking apoE-/- and LDLr-/- in combination with a high fat diet accelerates disease progression (2). While very similar to the natural mechanism, these methods are difficult to replicate due to the inherent variability of plaque behavior. One of the complexities to studying vulnerable plaques is that they do not produce a significant stenosis before they rupture and cause an acute MI. Additionally, some of the vulnerable plaques are short-lived and might resolve spontaneously. This plaque behavior makes its development hard to detect or track. Finally, it can be very complex to control the location or extent of MI when it occurs. Due to these difficulties with animal model disease-like-state recreation, interventional (surgery) models are often used.

There are two main interventional methods of MI induction in rodents, vascular occlusion and cryoinjury. Vascular occlusion can be used to either fully, partially or temporary restrict blood flow though a coronary artery. In rodents there are temporary occluders such as hanging weights (3), and different methods of permanent or temporary suture ligation (1, 4). There are also other methods for occlusion of coronary arteries mostly in large animals including: occluders (U-shaped, ring-shaped, ameroid constrictors), balloon inflation in coronary artery.

Currently the preferred method of introduction of MI in rodents is permanent suture ligation of the left descending coronary artery. The advantage of using permanent occlusion is that it mimics the behavior of a complete plaque blockage by inducing hypoxia and ischemia. It is important to note that rodent coronary arteries have different locations and branching patterns as compared to human coronary arteries (5, 6, and 7). For example, rats do not have the circumflex artery (8), therefore, the proximal region of the left coronary artery gives origin to the septal branch and to the branch that corresponds to the circumflex artery (9).

An alternative method to occlusion is creation of infarction by freeze-thaw injury (10) or cryoinjury (11, 12). This method allows for a specific region of tissue to be damaged unconstrained of coronary artery physiology. While this method has good reproducibility, it is less physiologically relevant as it causes tissue injury by different mechanism(s). This in turn impacts the response to infarct as seen by the delayed remodeling as compared to occlusion induced infarcts (12). Since a capable trained rodent surgeon is able to create permanent suture ligations with high reproducibility, using freeze-thaw or cryoinjury methods as MI induction model requires careful consideration for its translation and should be subjected to careful scrutiny before the project begins.

Translational Physiology of Myocardial Infarct Cont.

A common downside to artificially induced rodent myocardial infarcts is its relative low-emergence of other clinical symptoms associated with heart failure (pulmonary congestion, chest tightness, dyspnea, cachexia, ST-elevation myocardial infarction (STEMI) and non ST-elevation infarction (non-STEMI)). Additionally, there are a lack of rodent observational studies that pay specific attention to morbidity and mortality post-MI resulting from arrhythmias, cardiac rupture, heart failure, valve insufficiency, and embolization. As these comorbidities have the potential to alter the type, timing or extent of physiological responses, many rodent models are inherently limited in their clinical pathophysiology-translational bench-to bedside value.

CELLULAR AND GENETIC INFLUENCES

The heart's response to stresses such as MI is influenced, in part, by cellular phenotypic composition and genetics. For example, an adult mouse heart consists of approximately 45% non-cardiomyocytes and 55% cardiomyocytes, whereas adult rat and human hearts consists of around 70% of non-cardiomyocytes and 30% of cardiomyocytes (13). More studies are necessary to better characterize the two major cell types and their roles, including their intercellular interactions, during and post-MI. Without this knowledge it is very challenging to determine if and, to what extent heart, cellular composition affects cardiac behavior.

Genetic variations within species also factor into cardiovascular behavior as seen by strain-dependent difference in mortality rates. In a study by Liu *et. al.* the mortality of Sprague-Dawley rats was 36%, whereas in Lewis inbred rats it was significantly lower at 16% (14). Mice mortality associated with MI induction ranges from 37–50% (15). Furthermore, when different genetic backgrounds of mice were studied post-MI the highest incidence of post-MI infarct rupture, which typically occurred at 3–6 days post-MI, was in 129S6 mice (62%), followed by C57Bl6 (36%), FVB (29%), Swiss (23%), and BalbC (5%) (16). This incidence of high infarct rupture in 129S6 strain mice was associated with highest systolic blood pressure and presence of inflammation in the area. It must then be determined if those responses (high BP and inflammation) are physiologically accurate. Once the importance and relevance of genetically controlled comorbities are determined, they aid in choosing an appropriate translational model.

DISEASE RESPONSE BEHAVIOR

Equally important in mimicing a post-MI condition is having a meaningful biological response. In case of arrhythmias originating from post myocardial injury, there are differences between rodents and humans due to the dissimilar locations of major cardiac electrical axis. Different apoptosis progression, heart rate, and activity of various ionic channels also play a role in arrhythmias (17). However, the rat animal model can be ideal as compared to human in the assessment of various therapeutic interventions addressing arrhythmias due to a high frequency of ischemic ventricular arrhythmias in a repetitive, self-terminating manner (18).

Myocardial infarct size and LV chamber dilation are more pronounced in experimental rodent model systems as compared to human infarct. This adds an additional level of complexity to comparing infarct severity between species. According to the Killip-Kimball classification of infarct size on LV dysfunction, Class I is for small infarcts while Class IV is the most severe (the majority being fatal) with major necrosis involving more than 30% of the LV free wall. Similar pre-clinical classification of infarct size or method of correlating rodent infarct to the Killip-Kimball system is missing in animal models. This important classification can be incorporated into rodent models given the fact that rodent infarcts usually involve a much larger percentage of the cardiac tissue. At 21 days post-MI, rats with small MI (i.e. 4-30%) have no apparent impairment in baseline hemodynamics or peak indices of pumping and pressure generating ability when compared to the sham non-MI rats. Moderate MI between (31- 46%) is associated with normal baseline hemodynamics, but reduced peak flow indices and developed pressure. Large MI (46% and more) present congestive heart failure, with elevated filling pressures, reduced CO, and a minimal capacity to respond to pre- and afterload stresses (19). Note: In rodents the same percentage of infarct size (30%) which corresponds to severe in humans is classified as small, with minimal long term effects.

Translational Physiology of Myocardial Infarct Cont.

Remodeling behavior in rodents has some distinct differences as compared to humans. Post-MI cardiac remodelling in rodents is characterized by biventricular remodelling such that myocytes from the LV, RV and intra-ventricular septum are elongated to about the same extent, and thickness of septum increases (20). In humans, remodeling is centralized to the damaged ventricle.

CONCLUSION

The complex and multifaceted process of post myocardial infarct behavior precludes the study of a single animal model as being fully representative of the changes occurring in patients. Information combined from both large and small animal myocardial infarct models might help unravel key pathophysiological, cellular and gene mechanisms and provide the foundation for testing potential therapeutic strategies. Careful consideration of an experimental protocol increases its translational value.

REFERENCES

(1) Klocke R, Tian W, Kuhlmann MT, Nikol S. "Surgical animal models of heart failure related to coronary heart disease." Cardiovasc Res. 2007 Apr 1;74(1):29-38.

(2) Rosenfeld ME, Averill MM, Bennett BJ, Schwartz SM. "Progression and disruption of advanced atherosclerotic plaques in murine models." CurrDrug Targets. 2008;9:210 –216.

(3) Systematic Eckle T, Grenz A, Köhler D, Redel A, Falk M, Rolauffs B, Osswald H, Kehl F, Eltzschig HK. "Evaluation of a novel model for cardiac ischemic preconditioning in mice." Am J Physiol Heart Circ Physiol. 2006 Nov;291(5):H2533-40.

(4) Tarnavski O, McMullen JR, Schinke M, Nie Q, Kong S, Izumo S. "Mouse cardiac surgery: comprehensive techniques for the generation of mouse models of human diseases and their application for genomic studies." Physiol Genomics 16: 349–360, 2004.

(5) Salto-Tellez M, Yung Lim S, El-Oakley RM, Tang TP, Almsherqi ZA, Lim SK. "Myocardial infarction in the C57BL/6J mouse: a quantifiable and highly reproducible experimental model." Cardiovasc Pathol. 2004 Mar-Apr;13(2):91-7.

(6) Kumar D, Hacker TA, Buck J, Whitesell LF, Kaji EH, Douglas PS, Kamp TJ. "Distinct mouse coronary anatomy and myocardial infarction consequent to ligation." Coron Artery Dis. 2005 Feb; 16(1):41-4.

(7) Ahn D, Cheng L, Moon C, Spurgeon H, Lakatta EG, Talan MI. "Induction of myocardial infarcts of a predictable size and location by branch pattern probability-assisted coronary ligation in C57BL/6 mice." Am J Physiol Heart Circ Physiol. 2004 Mar; 286(3):H1201-7.

(8) Selye H, Bajusz E, Grassos S, Mendell P. "Simple techniques for the surgery occlusion of coronary vessels in the rat." Angiology. 1960; 11: 398-407.

(9) Spadaro J, Fishbein MC, Hare C, Pfeffer MA, Maroko PR. "Characterization of myocardial infarcts in the rat." Arch Pathol Lab Med. 1980; 104: 179-83.

(10) Taylor CB, Davis CB Jr, Vawter GF, Hass GM. "Controlled myocardial injury produced by a hypothermal method." Circulation 3: 239–253, 1951.

(11) Ciulla MM, Paliotti R, Ferrero S, Braidotti P, Esposito A, Gianelli U, Busca G, Cioffi U, Bulfamante G, Magrini F. "Left ventricular remodeling after experimental myocardial cryoinjury in rats." J Surg Res. 2004 Jan;116(1):91-7.

(12) van den Bos EJ, Mees BM, de Waard MC, de Crom R, Duncker DJ. "A novel model of cryoinjury-induced myocardial infarction in the mouse: a comparison with coronary artery ligation." Am J Physiol Heart Circ Physiol. 2005 Sep;289(3):H1291-300.

(13) Banerjee I, Fuseler JW, Price RL, Borg TK, Baudino TA. "Determination of cell types and numbers during cardiac development in the neonatal and adult rat and mouse." Am J Physiol Heart Circ Physiol. 2007;293: H1883–H1891.

(14) Liu YH, Yang XP, Nass O, Sabbah HN, Peterson E, Carretero OA. "Chronic heart failure induced by coronary artery ligation in Lewis inbred rats." Am J Physiol 1997;272:H722–7.

(15) Kuhlmann MT, Kirchhof P, Klocke R, Hasib L, Stypmann J, Fabritz L, Stelljes M, Tian W, Zwiener M, Mueller M, Kienast J, Breithardt G, Nikol S. "G-CSF/SCF reduces inducible arrhythmias in the infracted heart potentially via increased connexin43 expression and arteriogenesis." J Exp Med. 2006 Jan 23;203(1):87-97.

(16) van den Borne SW, van de Schans VA, Strzelecka AE, Vervoort-Peters HT, Lijnen PM, Cleutjens JP, Smits JF, Daemen MJ, Janssen BJ, Blankesteijn WM. "Mouse strain determines the outcome of wound healing after myocardial infarction." Cardiovasc Res. 2009 Nov 1;84(2):273-82.

(17) Wehrens XH, Kirchhoff S, Doevendans PA. "Mouse electrocardiography: an interval of thirty years." Cardiovasc Res. 2000 Jan 1;45(1):231-7.

(18) Opitz CF, Mitchell GF, Pfeffer MA, Pfeffer JM. "Arrhythmias and death after coronary artery occlusion in the rat. Continuous telemetric ECG monitoring in conscious, untethered rats." Circulation. 1995 Jul 15;92(2):253-61.

(19) Pfeffer MA, Pfeffer JM, Fishbein MC, Fletcher PJ, Spadaro J, Kloner RA, Braunwald E. "Myocardial infarct size and ventricular function in rats" Circ Res. 1979 Apr; 44(4):503-12.

(20) Zimmer HG, Gerdes AM, Lortet S, Mall G. "Changes in heart function and cardiac cell size in rats with chronic myocardial infarction." J Mol Cell Cardiol. 1990;22:1231–1243.

transonic
THE MEASURE OF BETTER RESULTS.

Hemodynamics of Cardiac Tissue Engineering

The heart has unique biomechanical properties. Each ventricular chamber (LV and RV) has a slightly different muscular/extracellular matrix (ECM) composition. The cellular composition of the heart also varies between species based on the amount of cardiomyocytes vs. supporting cells and on the amount and composition of the ECM (13). Studies show that cardiomyocytes behave poorly on man-made ECM surfaces (14). For that reason it is important to mimic the native cardiac mechanical environment.

The function of the supporting ECM is to stop or slow down the remodeling and scar formation process by preventing dilation of the heart muscle chambers. Meanwhile, delivered cells replace the dead cardiomyocytes/ supporting cells and integrate with the neighboring cardiac tissue. The supporting ECM should have niches to sustain the survival of the delivered cells to facilitate regeneration process.

The definitive objective of post-MI therapy is to attenuate the remodeling process and regenerate the new cardiomyocyte/support cell-based muscle. This can be achieved by a cell delivery system consisting of a supporting matrix and suitable cells. Currently, most strategies fail to address all the important factors for successful regeneration including: the loss of cardiomyocytes, attacks of inflammatory cells on unprotected vulnerable tissue, cell isolation and expansion, immunogenicity of grafted cells or matrix, cell survival, biomechanical/electrical coupling properties of the tissue constructs, cytotoxicity levels and degradation properties.

The active mechanical function of cardiac tissue is mostly delivered during systole. If the myocardium is replaced by a noncompliant scar tissue, systolic contraction is decreased. At the same time, not only contraction but also relaxation (diastole) is affected by the inability to accommodate all of the blood volume inside the cavity as the heart chamber stiffens. Using invasive PV hemodynamic assessment within stages of regenerative therapy, especially the load-independent parameters and contractility, increases the ability to properly measure and compare pathophysiological cardiac function.

As delivered cells have very low retaining capacity, researchers are making a variety of biomaterial scaffolds. Biomaterials often exhibit an intrinsic stiffness that may compromise diastolic function. Biodegradation of the scaffold material(s) often remains incomplete, adding to the potential problems with diastolic function.

Diastolic dysfunction (DD) is characterized by myocardium that has decreased ability to generate force and is unable to accept an adequate volume of blood during diastole at normal diastolic pressure. This results in an inability to maintain stroke volume (SV). Degradation of scaffold causes:

- Poor relaxation (impaired lusitropy)
- Decreased compliance

DD occurs when these scaffold degradation processes are prolonged, slowed and/or incomplete. DD generally depends on the onset, rate and extent of decline of pressure in ventricles and the relationship between pressure and volume, stress, or strain during diastole.

PV CHARACTERISTICS OF DD (LV LOAD-DEPENDENT MEASUREMENTS)

Representative PV loops of DD and diastolic failure can be found in “Understanding Lusitropy” on page 19

- LV EDP (end diastolic pressure) is increased with diastolic dysfunction as compared to healthy control. As the LV EDP rises left atrial and pulmonary venous pressures rise leading to pulmonary congestion and edema.
- Depending on the relative changes in SV and EDV, small decrease in EF and CO can be also observed. Because SV is decreased, decrease in ventricular SW can be also noticed on PV loop examination.
- Minimal/maximal rate of LV pressure change (dP/dt_{min}, dP/dt_{max}) is decreased.

Hemodynamics of Cardiac Tissue Engineering Cont.

PV CHARACTERISTICS OF DD (LV LOAD-INDEPENDENT MEASUREMENTS)

- EDPVR (end diastolic pressure volume relationship) represents relation between EDP-EDV points described by LV PV relationship. EDPVR is characterized by initial large increases in volume at low pressures. As volume increases further past the initial stage, pressure raises rapidly while volume increases slow as it is restrained by native ECM (e.g. collagen, proteoglycans, and glycoproteins). EDPVR curve fits are discussed in more depth in the publication by Burkhoff from 2005 (15). The EDPVR fits a non-linear curve that represents the diastolic stiffness (inverse of diastolic compliance) having the exponential fit EDP=A*exp (k*EDV), where k represents chamber stiffness or diastolic stiffness constant. K represents EDPVR slope, the change of ventricular pressure relative to a change in volume of the ventricular chamber (dP/dV).

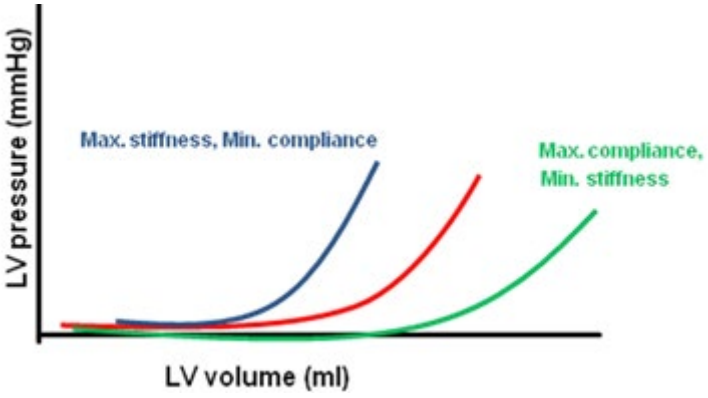

Representative drawings of EDPVR curves. Diastolic dysfunction (DD) impacts load independent properties of the left ventricle (EDPVR) during cardiac diastole characterized by the compliance and stiffness.

- When a tissue engineered construct is attached to the LV, compliance of the chamber often decreases. This overall chamber stiffening leads to a decrease of myocardial relaxation properties called lusitropy. Lusitropy is characterized by unwinding of individual sheets of myocardium proceeding into partial or complete relaxation. For more about lusitropy please see “Understanding Lusitropy” on page 19. The unique lusitropic properties of myocardium change during heart development and aging further challenging tissue construct site selection and final implantation.
- Isovolumic relaxation time (IVR) is the time from aortic valve closure to mitral valve opening. During DD, IVR might be prolonged. IVR or Tau (isovolumic pressure decay) is caused by uncoupling helically woven layers of myocardial fibers (including extracellular matrix) assembled in linked sheets. Myocardial fiber arrangement generates unique (heart specific) relaxation patterns which account for observed IVR pressure gradient during LV emptying and filling. Therefore, IVR (Tau) will increase post-cardiac patch implantation as compared to a non-injured heart. For more information about IVR please see “Understanding Lusitropy” on page 19.
- Ventricle elastance (Ees) describes the transmission of mechanical energy from the ventricle into the arterial system. Effective arterial elastance (Ea) can be derived from the ratio of ESP to SV (Ea = ESP/SV). A healthy arterial system works with maximum coupling efficiency, where Ees/ Ea = 0.3 to 1.3 (16). However, values outside of this range have to be thoroughly examined before deemed pathological. This unit-less ratio of coupling (Ees/ Ea) increases during diastolic insufficiency since both the systolic and diastolic ventricular efficiencies decline while there is an increase in afterload.

Hemodynamics of Cardiac Tissue Engineering Cont.

Difficulties and Considerations for Development of Functional Myocardium

CELL SOURCE & TYPE

CATEGORY	TYPE	LIMITATION
Source of cells	Autologous	Difficult to harvest in numbers
	Allogenic	Immunology roadblocks
	Xenogeneic	Rejections
	Syngeneic	Cloning, limited translational value
Type of cells	Harvested primary cells	Difficult to expand/organ specific
	Secondary from cryopreserved cell banks	Immunology roadblocks
	Adult stem cells	Source and type to use
	Embryonic stem cells	Purification, potential malignancy

AMOUNT & METHOD OF CELLS TO DELIVER

Some investigators use delivery of isolated stem cells (1-6); others use in vitro-designed tissue equivalents (7-10). Cells delivered without a scaffold (intravascular, intracoronary, intramyocardial, transendocardial, epicardial) are prone to large losses. Within minutes, 85-90% of cells injected intravascularly are lost, almost all cells are trapped in lungs (11) with less than 1% found in heart (12). While larger animal model cell-retention rates are usually higher, an optimal delivery method is still elusive.

Isolated stem cell (derived-cardiomyocytes, skeletal myoblasts, fibroblasts, mesenchymal, adipose stem cells etc.) delivered directly to the infarct site have low cell survival and poor cell engraftment, due to a lack of functional vasculature at the implant site, inflammation, and constant tissue remodeling (7, 17).

TIMING OF CELL DELIVERY

Timing of cell delivery is impacted by animal model/physiology and therapeutic target (limiting scar extension, limiting inflammation, improving angiogenesis, vascularization). The best timing of implanted cells delivery is still under discussion as all above-mentioned factors that are in play (1,5, 6, 8).

METHOD OF GROWING CELLS

Despite being able to grow functional cardiomyocytes in culture, the re-establishment of a contracting cardiac tissue (patch), including cardiac fibroblast and endothelial cells, is still elusive. Cardiac myocytes cultured in the standard 2D culture with the presence of growth-promoting medium lean towards de-differentiation and are often overgrown by non-myocytes. This has been largely overcome by using 3D culture environment. Additionally, the important influence of active or passive forces on cardiac myocyte growth, morphology, orientation, gene expression etc. has been demonstrated (7, 17). Substrates with a stiffness very close to that of the native adult rat myocardium were found to be favorable for heart cell morphology and function seen by cellular elongation, high contractile force and striations development (14).

Hemodynamics of Cardiac Tissue Engineering Cont.

TYPE OF SCAFFOLD

Most cardiac tissue engineering groups use scaffold proteins (e.g. collagen, gelatin, laminin, matrigel, hyaluronic acid (hyaluronan), alginate, and chitosan) or synthetic polymers (e.g. polylactic acid and polyglycolic acid) for tissue reconstitution from isolated cells.

Even the more common scaffolds, such as fibrin gel and matrigel, are far from ideal for cardiac tissue engineering. As the gelation rate of fibrin is slow and it lacks sufficient mechanical strength, there is a loss of delivered cells and low cell retention during injection. Its breakdown during heart contraction and relaxation is another downside along its high innate fibrinolysis rate. In case of matrigel, a biosafety concern exists, as it is derived from tumors (17).

Stabilization of the infarct area is the key concept for scaffold cellular delivery along with cell retention in the area. Temperature sensitive hydrogels mixed with variety of pro-angiogenic factors are a promising scaffold option (8).

SEEDING & GROWING CELLS ON SCAFFOLD

Tissue engineered cardiac patches (implanted tissue graft seeded with cardiomyocytes) have much less compact myocyte bundles as compared to native myocardium with less ability to generate necessary contractile force, often with non matured M bands. Core ischemia of the implanted graft seeded with cells often occurs. Cardiomyocytes incorporated on or in gelatin meshes form a thick cell layer only on the outside without a homogeneous cell distribution. Theoretical nutrient diffusion limit is 100-200 µm, but the limit is lower for more specialized cells such as cardiomyocytes (7). Substrate selection is also an important determinant of cell phenotypic development (14).

ELECTRICAL COUPLING

Despite observing implanted cell endurance and differentiation, mechanical and electrical cell-cell contacts between graft-and-host, required for synchronous contractions, are only rarely observed. Scar tissue appears to account for this problem by inhibiting contact between grafted cells and host tissue.

Inability to reproduce propagation of action potential (AP) is another concern. Action potential (current) propagates from SA (sinoatrial) pace-making node by intracellular channels (gap junctions). Most cells that are injected into the damaged SA node are not retained and might become pro-arrhytmic (18).

Hemodynamics of Cardiac Tissue Engineering Cont.

REFERENCES

(1) Li RK, Mickle DA, Weisel RD, Zhang J, Mohabeer MK. "In vivo survival and function of transplanted rat cardiomyocytes." Circ Res. 1996; 78: 283–288.

(2) Taylor DA, Atkins BZ, Hungspreugs P, Jones TR, Reedy MC, Hutcheson KA, Glower DD, Kraus WE. "Regenerating functional myocardium: improved performance after skeletal myoblast transplantation." Nat Med. 1998; 4: 929–933.

(3) Xaymardan M, Sun Z, Hatta K, Tsukashita M, Konecny F, Weisel RD, Li RK. 'Uterine cells are recruited to the infarcted heart and improve cardiac outcomes in female rats." J Mol Cell Cardiol. 2012 Jun;52(6):1265-73.

(4) Orlic D, Kajstura J, Chimenti S, Jakoniuk I, Anderson SM, Li B, Pickel J, McKay R, Nadal-Ginard B, Bodine DM, Leri A, Anversa P. "Bone marrow cells regenerate infarcted myocardium." Nature. 2001; 410: 701–705.

(5) Koh GY, Soonpaa MH, Klug MG, Pride HP, Cooper BJ, Zipes DP, Field LJ. "Stable fetal cardiomyocyte grafts in the hearts of dystrophic mice and dogs." J Clin Invest. 1995; 96: 2034–2042.

(6) Menasche P, Hagege AA, Scorsin M, Pouzet B, Desnos M, Duboc D, Schwartz K, Vilquin JT, Marolleau JP. "Myoblast transplantation for heart failure." Lancet. 2001; 357: 279–280.

(7) Zimmermann WH, Schneiderbanger K, Schubert P, Didié M, Münzel F, Heubach JF, Kostin S, Neuhuber WL, Eschenhagen T. "Tissue engineering of a differentiated cardiac muscle construct." Circ Res. 2002 Feb 8;90(2):223-30.

(8) Wu J, Zeng F, Huang XP, Chung JC, Konecny F, Weisel RD, Li RK. "Infarct stabilization and cardiac repair with a VEGF-conjugated, injectable hydrogel." Biomaterials. 2011 Jan;32(2):579-86.

(9) Didié M, Christalla P, Rubart M, Muppala V, Döker S, Unsöld B, El-Armouche A, RauT, Eschenhagen T, Schwoerer AP, Ehmke H, Schumacher U, Fuchs S, Lange C, BeckerA, Tao W, Scherschel JA, Soonpaa MH, Yang T, Lin Q, Zenke M, Han DW, Schöler HR, Rudolph C, Steinemann D, Schlegelberger B, Kattman S, Witty A, Keller G, Field LJ, Zimmermann WH. "Parthenogenetic stem cells for tissue-engineered heart repair." J Clin Invest. 2013 Mar 1;123(3):1285-98.

(10) Fujita J, Itabashi Y, Seki T, Tohyama S, Tamura Y, Sano M, Fukuda K. "Myocardial cell sheet therapy and cardiac function." Am J Physiol Heart Circ Physiol. 2012 Nov 15;303(10):H1169-82.

(11) Kraitchman DL, Tatsumi M, Gilson WD, Ishimori T, Kedziorek D, Walczak P, Segars WP, Chen HH, Fritzges D, Izbudak I, Young RG, Marcelino M, Pittenger MF, Solaiyappan M, Boston RC, Tsui BM, Wahl RL, Bulte JW. "Dynamic imaging of allogeneic mesenchymal stem cells trafficking to myocardial infarction." Circulation. 2005 Sep 6;112(10):1451-61.

(12) Barbash IM, Chouraqui P, Baron J, Feinberg MS, Etzion S, Tessone A, Miller L, Guetta E, Zipori D, Kedes LH, Kloner RA, Leor J. "Systemic delivery of bone marrow-derived mesenchymal stem cells to the infarcted myocardium: feasibility, cell migration, and body distribution." Circulation. 2003 Aug 19;108(7):863-8.

(13) Banerjee I, Fuseler JW, Price RL, Borg TK, Baudino TA. "Determination of cell types and numbers during cardiac development in the neonatal and adult rat and mouse." Am J Physiol Heart Circ Physiol. 2007;293: H1883–H1891

(14) Bhana B, Iyer RK, Chen WL, Zhao R, Sider KL, Likhitpanichkul M, Simmons CA, Radisic M. "Influence of substrate stiffness on the phenotype of heart cells." Biotechnol Bioeng. 2010 Apr 15;105(6):1148-60.

(15) Burkhoff D, Mirsky I, Suga H. "Assessment of systolic and diastolic ventricular properties via pressure-volume analysis: a guide for clinical, translational, and basic researchers." Am J Physiol Heart Circ Physiol. 2005 Aug;289(2):H501-12.

(16) De Tombe PP, Jones S, Burkhoff D, Hunter WC, Kass DA. "Ventricular stroke work and efficiency both remain nearly optimal despite altered vascular loading." Am J Physiol. 1993 Jun;264(6 Pt 2):H1817-24.

(17) Li Z and Guan J. "Hydrogels for Cardiac Tissue Engineering." Polymers 2011, 3(2), 740-761

(18) Macia E, Boyden PA. "Stem cell therapy is proarrhythmic." Circulation. 2009 Apr 7;119(13):1814-23.

transonic
THE MEASURE OF BETTER RESULTS.

Hemodynamic Assessment in Safety Pharmacology

Safety Pharmacology continues to be a rapidly developing discipline in a regulatory-driven process to generate data to inform risk/benefit assessment. In the cardiac field of study the aim of Safety Pharmacology (SP) is to characterize the pharmacodynamic/pharmacokinetic (PK/PD) relationship of a drug's adverse effects in the heart and circulation. Unlike toxicology, safety pharmacology includes a regulatory requirement to predict the risk of rare lethal events such as torsades de pointes (TdP) syndrome.

IMPORTANCE OF CARDIAC HEMODYNAMIC ASSESSMENT IN DRUG DISCOVERY AND EVALUATION

As an example of the importance of testing for potential adverse cardiovascular effects, in the mid 1990's the antihistamine, terfenadine (Seldane), was withdrawn following a growing awareness that the drug could evoke the potentially life threatening cardiac syndrome, torsades de pointes (TdP) or polymorphic ventricular tachycardia, in otherwise healthy patients (1). TdP reaction from this antihistamine only became evident after several millions of prescriptions, put many people at risk. This incident, and others like it in the late 1980s and early 1990s, gave rise to specialization of safety pharmacology, which was not previously recognized as very relevant. From this came safety testing for cardiovascular impact of non-cardiovascular drugs consisting of the evaluation of QT interval prolongation to screen for TdP liability.

Recent SP approaches using ECG measurements include measurements of QT interval as a surrogate biomarker of cardiac biopotentials (1, 2, and 9). For example, non-cardiovascular indicated drugs such as droperidol, lidoflazine, and cisapride were removed from market solely based on the QT interval. Clinicians are constantly faced with both older and newly approved drugs labelled as potentials for TdP. While at the same time drugs considered to be safe in non-clinical studies may be found to have QT-liability (proarrhythmic risk) in early clinical studies (2). Regulatory authorities might ask for scientific rationalization for this incongruity and, as long as the safety of subjects in later phase clinical trials is assured, the sponsor may then decide whether to continue or terminate the drug development in light of the risks.

SAFETY PHARMACOLOGY GUIDELINES

The S7A: Safety Pharmacology Studies for Human Pharmaceuticals guideline for the conduct of safety pharmacology evaluations recommends using a core battery of studies on three vital organ systems (cardiovascular, respiratory and central nervous system) to assess the potential risks of novel pharmaceuticals for human use.

Core Cardiovascular Studies:

- Central arterial pressure
- Heart rate
- Electrocardiogram (ECG)
- Electrophysiology (hERG)

Supplemental Cardiovascular Studies:

- Cardiac output
- Ventricular contractility
- Ventricular resistance

TRADITIONAL METHODS OF ASSESSMENT IN PRE-CLINICAL SAFETY PHARMACOLOGY

Cardiac and hemodynamic studies have the potential for significant variation between investigators as the ability to detect adverse effects is subjective and sometimes inconsistent. For detecting adverse effects of tested (candidate) drug on cardiac contractility, pre-clinical safety pharmacology mostly uses a combination of ECG with a pressure catheter to study QA interval compared with LV dP/dt max (Fig 1). This set up allows for a two-index comparison of heart contractility to assess the inotropic induction (3, 4 and 5). The QA interval covers the period of time of initial depolarization of ventricles (R decline) until the time when the aortic valve opens. For the purpose of determining the QA interval, the time between the Q on the ECG and the beginning of the upstroke on the arterial blood pressure is used as an indicator of altered LV contractility (Fig. 1). Drugs that slow conduction velocity through the heart could prolong the QA, and may have more effect on QA than on LV dP/dt max. Theoretically, reduction of blood pressure induced by the candidate drug causing reduced arterial stiffness might reduce pulse wave propagation and thus QA interval. Moreover, QA captures reduced contractility more precisely than compared to increased contractility.

Hemodynamic Assessment in Safety Pharmacology Cont.

Other safety pharmacologists use the LV dP/dt max-HR relationship to determine the force-frequency relationship while singling out LV dP/dt max as a measure of pharmacodynamic heart contractility endpoint (6). It is important to note that many drugs induce both chronotropic and inotropic effects which changes HR along with LV dP/dt max and that LV dP/dt max changes with HR. Thus changes to contractility must be evaluated based on the corresponding changes in heart rate (6).

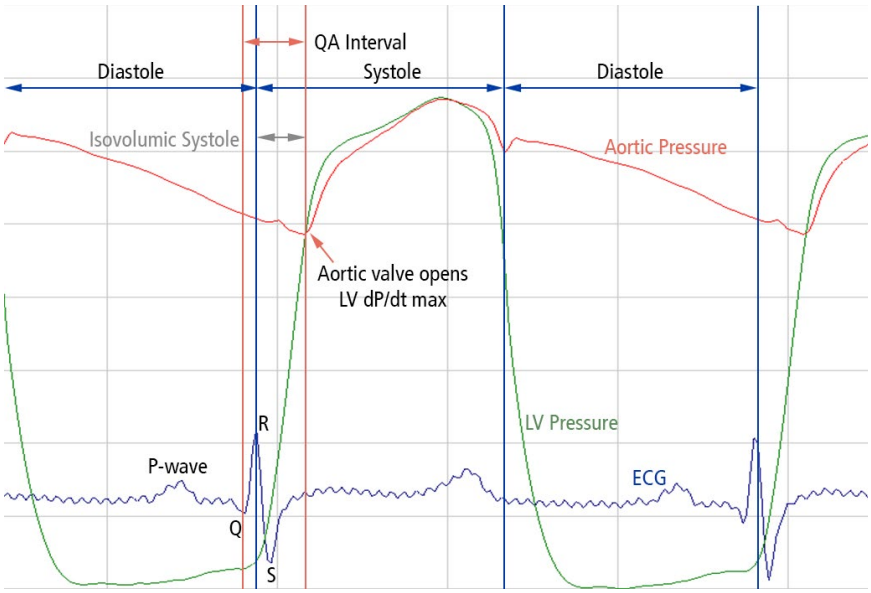

Fig. 1: QA interval approximates of the average rate of isovolumic systolic pressure development.

PV LOOPS IN PRE-CLINICAL SAFETY PHARMACOLOGY

Recently, Conductance and Admittance PV loop technology has been used for screening and pharmacologic assessment of the inotropic state of the heart (7,8). While this method is the gold standard for investigation of cardiac function with respect to clinical disease, it is currently not widely used in safety pharmacology (7). By using the relationship of pressure and volume for interrogation of the LV, safety pharmacologists can better determine lusitropic effects of myocardial relaxation that cannot be otherwise captured by using two indices comparison (e.g. QA interval with LV dP/dt max). Moreover, other important parameters of load independent measurements such as ESPVR, EDPVR, PRSW, PVA can be determined, strengthening conclusions about the tested drug candidate.

REFERENCES

(1) Monahan BP, Ferguson CL, Killeavy ES, Lloyd BK, Troy J, Cantilena LR., Jr "Torsades de pointes occurring in association with terfenadine use." JAMA. 1990;264:2788–2790.

(2) Shah RR. "If a drug deemed 'safe' in nonclinical tests subsequently prolongs QT in phase 1 studies, how can its sponsor convince regulators to allow development to proceed?" Pharmacol Ther. 2008 Aug;119(2):215-21.

(3) Mooney L, Marks L, Philp KL, Skinner M, Coker SJ, Currie S. "Optimising conditions for studying the acute effects of drugs on indices of cardiac contractility and on haemodynamics in anaesthetized guinea pigs." J Pharmacol Toxicol Methods. 2012 Jul;66(1):43-51.

(4) Johnson DM, Geys R, Lissens J, Guns PJ. "Drug-induced effects on cardiovascular function in pentobarbital anesthetized guinea-pigs: invasive LVP measurements versus the QA interval." J Pharmacol Toxicol Methods. 2012 Sep;66(2):152-9.

(5) Norton K, Iacono G, Vezina M. "Assessment of the pharmacological effects of inotropic drugs on left ventricular pressure and contractility: an evaluation of the QA interval as an indirect indicator of cardiac inotropism." J Pharmacol Toxicol Methods. 2009 Sep-Oct;60(2):193-7.

(6) Markert M, Trautmann T, Groß M, Ege A, Mayer K, Guth B. "Evaluation of a method to correct the contractility index LVdP/dt(max) for changes in heart rate." J Pharmacol Toxicol Methods. 2012 Sep;66(2):98-105.

(7) Marks L, Borland S, Philp K, Ewart L, Lainée P, Skinner M, Kirk S, Valentin JP. "The role of the anaesthetised guinea-pig in the preclinical cardiac safety evaluation of drug candidate compounds." Toxicol Appl Pharmacol. 2012 Sep 1;263(2):171-83.

(8) Violin JD, DeWire SM, Yamashita D, Rominger DH, Nguyen L, Schiller K, Whalen EJ, Gowen M, Lark MW. "Selectively engaging β-arrestins at the angiotensin II type 1 receptor reduces blood pressure and increases cardiac performance." J Pharmacol Exp Ther. 2010 Dec;335(3):572-9.

(9) Authier S, Gervais J, Fournier S, Gauvin D, Maghezzi S, Troncy E. "Cardiovascular and respiratory safety pharmacology in Göttingen minipigs: Pharmacological characterization." J Pharmacol Toxicol Methods. 2011 Jul-Aug;64(1):53-9.

Right Ventricle Pressure-Volume Loops

As hemodynamic assessment techniques progress, RV pathology can be better characterized including assessing changes from a healthy to a compensated (hypertrophied) condition and then decompensated condition. Cardiac catheterization remains the best method to diagnose pulmonary hypertension, assess disease severity, and determine prognosis and response to therapies. By directly measuring pressures and volumes, right heart catheterization allows determination of prognostic systolic indices, diastolic indices, pulmonary vascular indices and the coupling ratio. For more information about using right ventricular PV loops to study pulmonary artery hypertension see: "Pulmonary Artery Hypertension & RV PV Loops" on page 19.

Primarily, RV function may be impaired due to:

- Primary right side heart disease
- Secondary LV issues
- Heart valve disease (RV or LV)
- Post-reparative changes from congenital heart disease (e.g. Fallot tetralogy, pulmonary stenosis, insufficiency)
- Post-correction of hypoplastic left heart syndrome
- Arterio-caval shunt (increased afterload)

RV dysfunction may affect LV function by:

- Limiting LV preload
- Systolic and diastolic interaction through intra-ventricular septum
- Pericardium ventricular interdependence by constraints of heart pericardium post-inflammation

METHODS FOR ASSESSING RV HEMODYNAMICS

Non-Invasive Methods:

- Echocardiography (2D or 3D)
- Tissue Doppler imaging (TDI)
- Magnetic resonance imaging (MRI)
- Computed (large animals) or Micro-computed (rodents) Tomography; CT or micro-CT

Invasive Methods:

- Virtual pressure-volume loops (MRI and Pressure)
- Catheter measurement of pulmonary artery pressure (PAP), Right ventricular (RVP) and right atrial pressures (RAP).
- Pressure Catheter combined with Perivascular Flowprobe
- Right ventricle pressure volume (RV-PV) loops (Pressure-volume catheter)

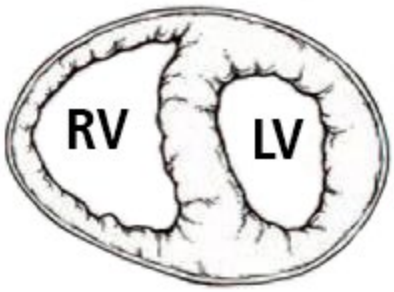

The anatomical and physiological characteristics of a typical right ventricle is complex. Compared to the ellipsoidal LV shape, the RV appears triangular when viewed from the side and crescent shaped when viewed in cross section (above). The RV shape is also influenced by the position of the inter-ventricular septum. Under normal loading and electrical conditions, the septum is concave toward the LV in both systole and diastole. RV has different genetic composition as compared to the LV, making it vulnerable when hypertrophied due to its septomarginal muscular band, which can divide the ventricle into 2 chambers (double-chambered RV). Additionally, the volume of the RV is larger than the volume of the LV, whereas RV mass is approximately one sixth that of the LV. This allows better accommodation of volume but not pressure. A sudden increase in RV pressure is deadly, as compared to a slow afterload increase since RV adaptation occurs at a slower pace.

Figure from Champion HC, et. al. "Comprehensive Invasive and Noninvasive Approach to the Right Ventricle–Pulmonary Circulation Unit: state of the art and clinical and research implications." Circulation. 2009 Sep 15;120(11):992-1007

Right Ventricle Pressure-Volume Loops Cont.

METHODS FOR ASSESSING RV HEMODYNAMICS CONT.

Each method has advantages and limitations so it is important to consider what parameters are of interest, study methodology requirements, equipment requirements and cost, measurement time, difficulty and repeatability. For a comparison between Echocardiography, PV Catheterization, CT and MRI see "Introduction: Cardiac Volume Measurement Methods" on page 2.

Note: Major difficulties of basic RV 2D echocardiography as compared to the basic LV 2D echo include:

- Inadequate formula to characterize RV volume based on the RV shape. Current formulas specific to the LV.
- As the RV has thinner walls and chamber has more trabeculations as compared to the LV, it is more complex to echocardiographically characterize it.
- An acoustic barrier is created by its retrosternal position.

RIGHT VENTRICLE PRESSURE-VOLUME LOOP CHARACTERISTICS AS COMPARED TO THE LEFT VENTRICLE

- EDPVR of the RV is characterized by its high compliance (compliance is increased) as compared to LV.
- At any given end-diastolic volume (EDV) the RV end-diastolic pressure (EDP) is lower, making the final EDPVR shallower as compared to the LV.
- Ejection of blood into the highly compliant, low-resistance pulmonary circulation results in better coupling (Ees/Ea).
- Normal RV generates less than 20% of the stroke work (SW) of the LV while moving the same volume of blood. Compared to LV, a much lower proportion of RV SW goes to pressure generation as compared to LV.

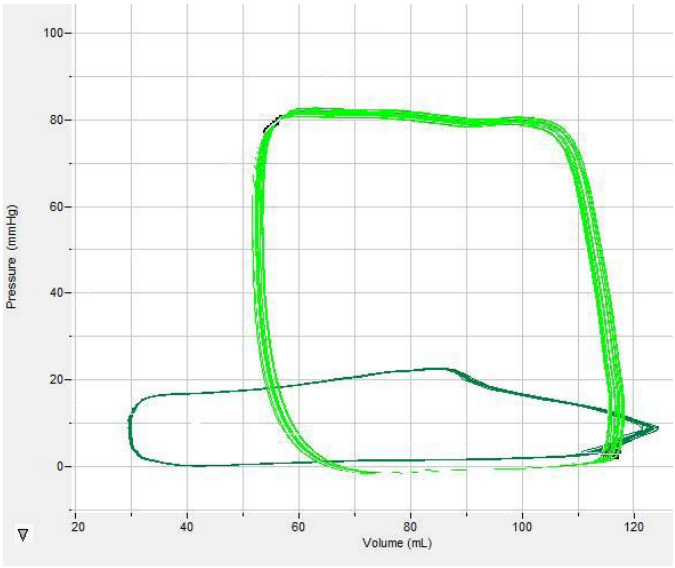

Pressure-Volume loops during steady state recording. Images are taken from the same sheep heart. Dark green PV loops represent RV steady state, while light green are LV PV loops.

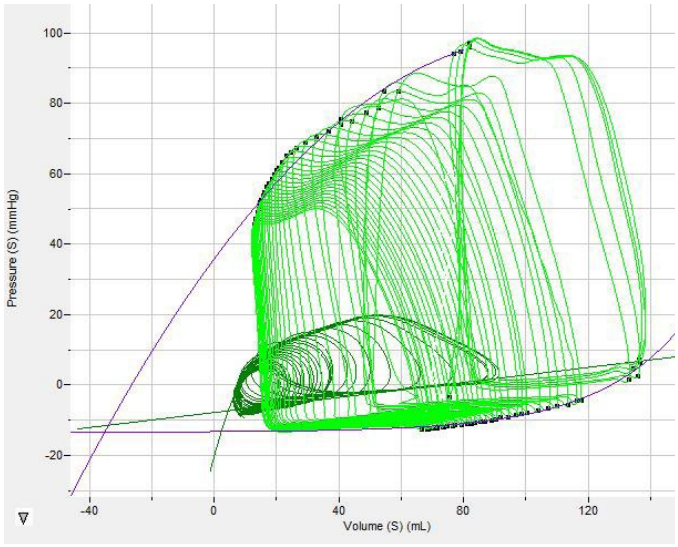

Pressure-Volume loops during IVC occlusion. Images are taken from the same pig heart. Dark green PV loops represent RV, while light green are LV PV loops post-IVC occlusion.

Right Ventricle Pressure-Volume Loops Cont.

RIGHT VENTRICLE PRESSURE-VOLUME LOOP CHARACTERISTICS AS COMPARED TO THE LEFT VENTRICLE CONT.

- The RV accommodates dramatic variations in venous return resulting from changes in volume status, position, and respiration while maintaining more or less constant cardiac output (CO). In part this is because the thin RV is easily distensible, but to a larger extent it is a direct result of RV geometry. Like the LV, the RV utilize the Frank-Starling mechanism to increase SW as a consequence of an increase in RV stretch, but much larger changes in RV volume are needed before the Frank-Starling mechanism is engaged.
- The RV coronary perfusion pattern significantly differs from that of the LV. Because tissue pressure in the LV rises during systole to systemic levels, coronary perfusion of the LV is largely confined to the diastolic interval. Tissue pressure in the RV does not normally exceed aortic root systolic pressure, permitting continued coronary flow throughout the cardiac cycle. Thus, under typical hemodynamic conditions, coronary flow to the RV is roughly balanced between systolic and diastolic time periods.

RV INDICES IN MICE (Tabima et. al. 2010)			
INDICES	**HEALTHY RV**	**HYPERTROPHIED RV**	**FORMULA**
Heart rate (HR)	611 ± 31 bpm	636 ± 31 bpm	
RV Systolic pressure	27 ± 3 mmHg	45 ± 17 mmHg	
RV Diastolic pressure	1.4 ± 0.9 mmHg	2.7 ± 1.4 mmHg	
RV Stroke work (SW)	386 ± 76 mmHg*µL	926 ± 265 mmHg*µL	SV*MAP
RV Cardiac output (CO)	8.5 ± 2.3 ml/min	5.2 ± 2.6 ml/min	SV*HR
RV Stroke volume (SV)	13.9 µL	8.2 µL	CO/HR (EDV-ESV)
Ejection Fraction (EF)	51 ± 11%	28 ± 13%	SV/EDV*100
Mean Arterial pressure (MAP)	27.8 mmHg	112.9 mmHg	SW/SV
dP/dt_{max}	2522 ± 660 mmHg/s	3164 ± 826 mmHg	
dP/dt_{max} - end-diastolic volume	84 ± 17 mmHg/s/µL	177 ± 93 mmHg/s/µL	dP/dt_{max} vs. EDV
dP/dt_{min}	-1971 ± 499 mmHg/s	-3009 ± 1120 mmHg/s	
Preload recruitable stoke work (PRSW)	20.9 ± 5.6 mmHg	33.9 ± 5.9 mmHg	SW vs. EDV
Ventricular end-systolic elastance (Ees)	1.8 ± 0.5 mmHg/µL	2.4 ± 0.2 mmHg/µL	ESP/ESV
Effective arterial elastance (Ea)	2.7 ± 1.2 mmHg/µL	16.4 ± 2.5 mmHg/µL	ESP/SV
Coupling ratio: Ees/Ea	0.71 ± 0.27 Optimal > 0.5	0.35 ± 0.17 Uncoupled < 0.5	SV/ESV

REFERENCES

Andersen A, et. al. "Effects of phosphodiesterase-5 inhibition by sildenafil in the pressure overloaded right heart." Eur J Heart Fail. 2008 Dec;10(12):1158-65.

Bartelds B, et. al. "Bartelds Differential responses of the right ventricle to abnormal loading conditions in mice: pressure vs. volume load." Eur J Heart Fail. 2011 Dec;13(12):1275-82.

Blaudszun G, Morel DR. "Superiority of desflurane over sevoflurane and isoflurane in the presence of pressure-overload right ventricle hypertrophy in rats." Anesthesiology. 2012 Nov; 117(5): 1051-61.

Boissiere J, et. al. "Doppler tissue imaging in assessment of pulmonary hypertension-induced right ventricle dysfunction." Am J Physiol Heart Circ Physiol. 2005 Dec;289(6):H2450-5.

Fitzpatrick JM, Grant BJ. "Effects of pulmonary vascular obstruction on right ventricular afterload." Am Rev Respir Dis. 1990 Apr;141:944-52.

Kumar S, et. al. "Cardiac-specific genetic inhibition of nuclear factor-κB prevents right ventricular hypertrophy induced by monocrotaline." Am J Physiol Heart Circ Physiol. 2012 Apr 15; 302(8): H1655-66.

Piao L, et. al. "GRK2-mediated inhibition of adrenergic and dopaminergic signaling in right ventricular hypertrophy: therapeutic implications in pulmonary hypertension." Circulation. 2012 Dec 11; 126(24): 2859-69.

Tabima DM, Hacker TA, Chesler NC. "Measuring right ventricular function in the normal and hypertensive mouse hearts using admittance-derived pressure-volume loops." Am J Physiol Heart Circ Physiol. 2010 Dec; 299(6): H2069-75.

transonic
THE MEASURE OF BETTER RESULTS.

Pulmonary Artery Hypertension & RV PV Loops

PULMONARY HYPERTENSION AND RIGHT VENTRICLE REMODELING

The pulmonary circulation has shorter arteries and veins, more distensible (high compliant and low resistant) large arteries, and a larger number of peripheral arteries as compared to the systemic circulation. This leads to RV afterload being significantly lower than LV afterload and matching ventricular-vascular coupling. Pulmonary hypertension (PH) is diagnosed when mean pressure in the pulmonary artery increases over a threshold. Pulmonary artery hypertension (PAH) is a subtype of PH classification defined as a mean pulmonary artery pressure (PAP) greater than 25 mmHg with peak pressure greater than 33 mmHg at rest or mean PAP greater than 30 mmHg during exercise (1, 19). Other clinically distinct PH causes include: PH owing to the left heart disease, PH owing to lung disease or hypoxia, and chronic thromboembolic PH (CTEPH).

PAH is important subtype of PH as it originates when pulmonary arteries muscularize while its vascular media hypertrophies, leading to a progressive narrowing of the arterial lumen. It is a syndrome in which obstruction of pulmonary arteries increases pulmonary vascular resistance (PVR) leading to right ventricular (RV) hypertrophy (20). Its etiology is not completely understood at this time, as multiple factors are involved. Vascular pathology changes induced by PH are characterized by intimal thickening and fibrosis, medial hypertrophy, muscularization of previously non-muscularized arteries, adventitial proliferation and increased extracellular matrix (ECM) deposition (8). PAH is responsible for proximal pulmonary artery stiffening (changes of PA pulsatility, compliance, capacitance, distensibility, elastic modulus, and pressure-independent stiffness index beta) (2) and RV dysfunction (18). RV has to accommodate (the compensatory changes) an increased afterload due to the PA pressure elevation or it will fail.

Experimental models of pulmonary hypertension include direct damage of pulmonary endothelial cells (EC) by monocrotalin, alpha-napthyltiourea, microspheres, Angiopoetin-1, or Bleomycin, and subsequent EC and vascular smooth muscle cells proliferation in the area (19). In this context, RV autoregulation changes promote a temporary increase in RV contractility. During this condition, elevated wall stresses develop in the RV lateral free wall (4) and outflow tract (5). Increased wall stresses from increased mean pressure in the PA and increased pulmonary vascular resistance (PVR) further stimulate RV hypertrophy (5) and RV free wall fibrosis (6).

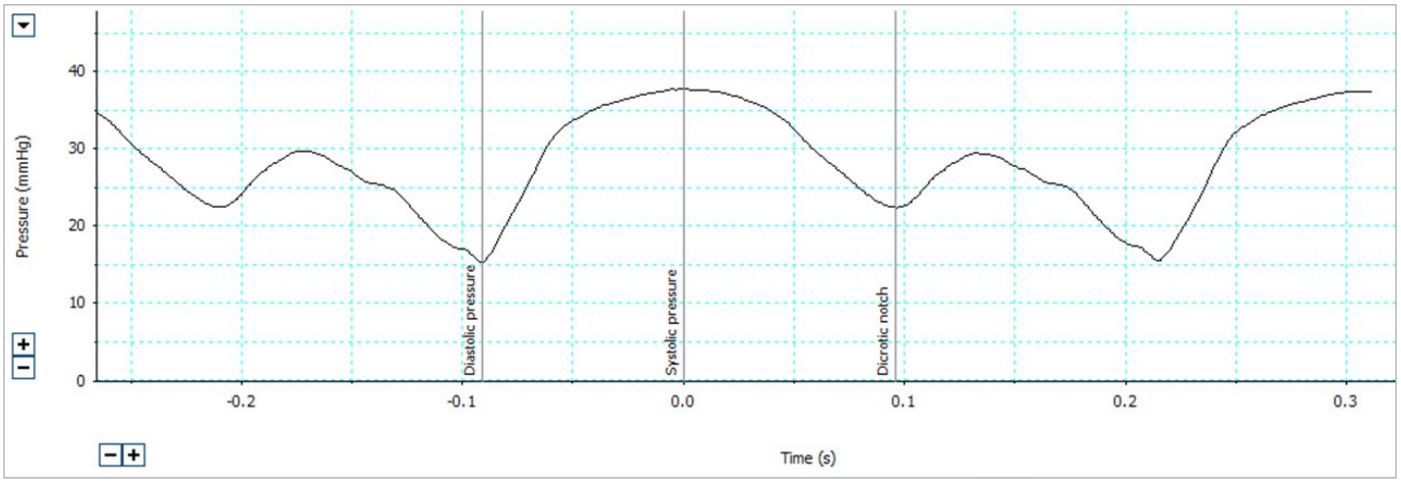

Fig. 1: Pressure trace in pig pulmonary artery during hypertension. Peak pressure is over 35 mmHg at rest.

Pulmonary Artery Hypertension & RV PV Loops Cont.

ASSESSMENT OF RIGHT VENTRICLE POST PAH USING RV PV LOOPS

Based on experimental data obtained from mouse RV pressure-volume study of PAH injury, models of the ventricular mechanics showed increasing RV afterload while effectively putting strain on the RV. The models show that vascular resistance, arterial elastance and arterial narrowing all play important roles in final RV remodeling (21).

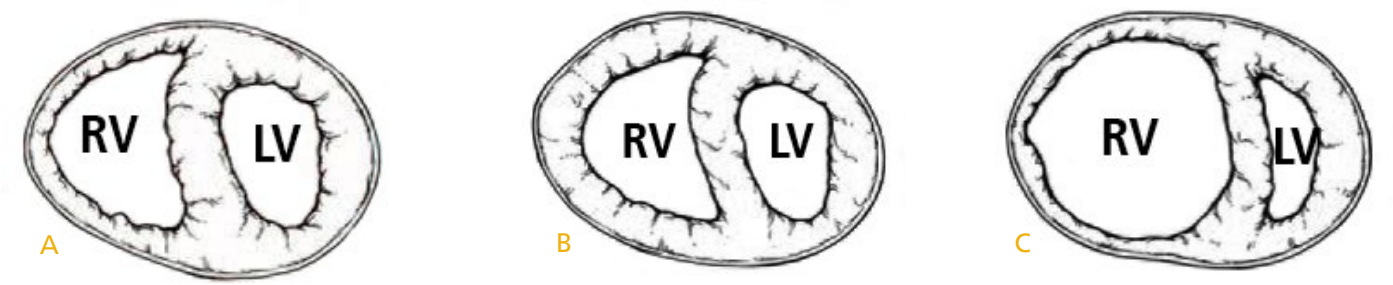

Fig. 2: A) Intact Rigth Ventricle B) PAH compensatory changes are responsible for RV free wall hyperthrophy which temporarily protects RV cardiac output and stroke volume. Heart rate might temporarily increase. RV afterload increases without significant volume changes (Fig. 3A). As PAH progresses changes in RV chamber volume occur (Fig. 3B) C) Right Ventricle dilates and fails, decrease in stroke work, stroke volume, cardiac output, and ejection fraction (Fig. 3C). Figures from Champion HC, et. al. Comprehensive Invasive and Noninvasive Approach to the Right Ventricle–Pulmonary Circulation Unit: state of the art and clinical and research implications. Circulation. 2009 Sep 15;120(11):992-1007

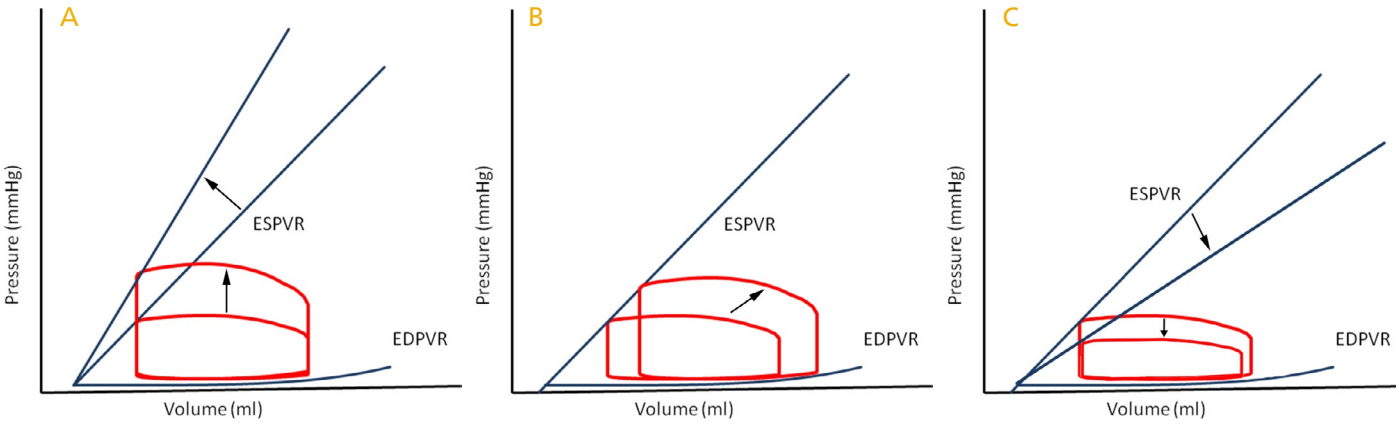

Fig. 3: Representative drawing of RV PV loops post PAH. A) Represents situation of PAH where temporary increase of pressure in the PA (increase of after-load) can be detected in the RV PV loop without volume changes. B) Represents compensatory changes of RV (increase of after-load) where both pressure and volumes changes during PAH. C) Represents failing RV as chamber dilates which is marked by decrease of stroke work, cardiac output and ejection fraction and other key parameters.

ASSESSMENT OF RIGHT VENTRICLE POST PAH USING RV PV LOOPS CONT.

In the mouse, the onset of PAH is characterized by significant RV ESP increase. During early PAH the right ventricle increases its efficiency during systole to meet an increasing afterload, but as PAH progresses, its work efficiency plateaus (Fig. 3A) (22). During diastole RV EDV increases, suggesting a larger RV compliance, but in fact, as RV EDP increases, it also makes the RV chamber stiffer in diastole and that is most likely a consequence of RV wall stiffening (22). Because increased RV EDV is a strong predictor of mortality in PAH (7) detection of changes using pressure-volume measurements are very important.

Since the mechanism(s) and factors involved in the transition from an adaptive hypertrophy to maladaptive remodelling are currently unknown, a comprehensive study of RV hemodynamics is valuable. More research is underway to assess RV hemodynamics, energy balance, LV-RV dysynchrony and other possible mechanisms leading to

Pulmonary Artery Hypertension & RV PV Loops Cont.

this progressive RV failure and multiple studies in recent years used RV PV loops in their pulmonary hypertension research (9-17). For an excellent in-depth review of *in-vivo* measurements and detection of stiffening of the PA influencing the RV hemodynamics in clinical, large animal and small animal setting, please refer to an article by Chesler & Tian (18).

Historically, RV mass measured by non-invasive magnetic resonance imaging has been used as an indication of RV dysfunction due to PAH. This method, however, is not considered a strong predictor of mortality, and for this reason, this finding cannot be fully translated into the clinic (7). This disconnect between mass and mortality is possibly due to an adaptive remodelling, known also as a concentric hypertrophy without dilation happening in the RV post PAH. This leads to more longitudinal monitoring of RV pressure and volume during PAH.

One of the first uses of 5F and 6F Conductance Catheters was described by Dickstein *et. al.* in 1995. This group measured volume in the RV and correlated data to flow derived volumes measured by 16 mm Transonic Flowprobe placed on the pulmonary artery (3). The advances of Admittance technology reduces the geometric dependence of PV measurements and has allowed for right ventricular pressure-volume measurements to be more precise (15, 16).

REFERENCES

(1) Simonneau G, et. al. "Updated clinical classification of pulmonary hypertension." J Am Coll Cardiol. 2009 Jun 30;54(1 Suppl):S43-54.

(2) Sanz J, et. al. "Evaluation of pulmonary artery stiffness in pulmonary hypertension with cardiac magnetic resonance." JACC Cardiovasc Imaging. 2009 Mar;2(3):286-95

(3) Dickenstein ML, et. al. "Assessment of right ventricular contractile state with the conductance catheter technique in the pig." Cariovasc. res 1995; 29:820-6

(4) Quaife RA, et. al. "Importance of right ventricular end-systolic regional wall stress in idiopathic pulmonary arterial hypertension: a new method for estimation of right ventricular wall stress." Eur J Med Res. 2006 May 5;11(5):214-20.

(5) Simon MA, et. al. "Phenotyping the right ventricle in patients with pulmonary hypertension." Clin Transl Sci. 2009 Aug;2(4):294-9.

(6) Sanz J, et. al. "Prevalence and correlates of septal delayed contrast enhancement in patients with pulmonary hypertension." Am J Cardiol. 2007 Aug 15;100(4):731-5.

(7) van Wolferen SA, et. al. "Prognostic value of right ventricular mass, volume, and function in idiopathic pulmonary arterial hypertension." Eur Heart J. 2007 May; 28(10):1250-7.

(8) Stenmark KR, et. al. "The adventitia: essential role in pulmonary vascular remodeling." Compr Physiol. 2011 Jan;1(1):141-61.

(9) Wagenaar GT, et. al. "Ambrisentan reduces pulmonary arterial hypertension but does not stimulate alveolar and vascular development in neonatal rats with hyperoxic lung injury." Am J Physiol Lung Cell Mol Physiol. 2013 Feb 15;304(4):L264-75.

(10) Cavasin MA, et. al. "Selective class I histone deacetylase inhibition suppresses hypoxia-induced cardiopulmonary remodeling through an antiproliferative mechanism." Circ Res. 2012 Mar 2;110(5):739-48.

(11) Umar S, et. al. "Allogenic stem cell therapy improves right ventricular function by improving lung pathology in rats with pulmonary hypertension." Am J Physiol Heart Circ Physiol. 2009 Nov;297(5):H1606-16.

(12) Kumar S, et. al. "Cardiac-specific genetic inhibition of nuclear factor-κB prevents right ventricular hypertrophy induced by monocrotaline." Am J Physiol Heart Circ Physiol. 2012 Apr 15;302(8):H1655-66.

(13) Wang Z, et. al. "Effects of collagen deposition on passive and active mechanical properties of large pulmonary arteries in hypoxic pulmonary hypertension." Biomech Model Mechanobiol. 2013 Nov;12(6):1115-25.

(14) Nagendran J, et. al. "Endothelin axis is upregulated in human and rat right ventricular hypertrophy." Circ Res. 2013 Jan 18;112(2):347-54.

(15) Tabima DM, et. al. "Measuring right ventricular function in the normal and hypertensive mouse hearts using admittance-derived pressure-volume loops." Am J Physiol Heart Circ Physiol. 2010 Dec;299(6):H2069-75.

(16) Schreier D, et. al. "The role of collagen synthesis in ventricular and vascular adaptation to hypoxic pulmonary hypertension." J Biomech Eng. 2013 Feb;135(2):021018.

(17) Yasuda T, et. al. "Rho-kinase inhibition alleviates pulmonary hypertension in transgenic mice expressing a dominant-negative type II bone morphogenetic protein receptor gene." Am J Physiol Lung Cell Mol Physiol. 2011 Nov;301(5):L667-74.

(18) Tian L, Chesler NC. "In vivo and in vitro measurements of pulmonary arterial stiffness: A brief review. "Pulm Circ. 2012 Oct;2(4):505-17.

(19) Marsboom GR, Janssens SP. "Models for pulmonary hypertension. Drug Discovery Today Disease models." 2004 1(3): 289-96.

(20) Ciuclan L, et. al. "A novel murine model of severe pulmonary arterial hypertension." Am. J. Respir.Crit.CareMed. 2011: 184, 1171–1182.

(21) Tewari SG, et. al. "Analysis of cardiovascular dynamics in pulmonary hypertensive C57BL6/J mice." Front in Physiol 2013 Dec; (4), 1-9

(22) Wang Z,et. al. "Progressive right ventricular functional and structural changes in a mouse model of pulmonary arterial hypertension." Physiol Rep, 1 (7), 2013.

transonic
THE MEASURE OF BETTER RESULTS.

www.transonic.com

Transonic Systems Inc. is a global manufacturer of innovative biomedical measurement equipment. Founded in 1983, Transonic sells "gold standard" transit-time ultrasound flowmeters and monitors for surgical, hemodialysis, pediatric critical care, perfusion, interventional radiology and research applications. In addition, Transonic provides pressure and pressure volume systems, laser Doppler flowmeters and telemetry systems.

AMERICAS
Transonic Systems Inc.
34 Dutch Mill Rd
Ithaca, NY 14850
U.S.A.
Tel: +1 607-257-5300
Fax: +1 607-257-7256
support@transonic.com

EUROPE
Transonic Europe B.V.
Business Park Stein 205
6181 MB Elsloo
The Netherlands
Tel: +31 43-407-7200
Fax: +31 43-407-7201
europe@transonic.com

ASIA/PACIFIC
Transonic Asia Inc.
6F-3 No 5 Hangsiang Rd
Dayuan, Taoyuan County
33747 Taiwan, R.O.C.
Tel: +886 3399-5806
Fax: +886 3399-5805
support@transonicasia.com

JAPAN
Transonic Japan Inc.
KS Bldg 201, 735-4 Kita-Akitsu
Tokorozawa Saitama
359-0038 Japan
Tel: +81 04-2946-8541
Fax: +81 04-2946-8542
info@transonic.jp

PV Workbook RPV-4-wb Rev A 2014